CORROSION TESTING OF HIGH TEMPERATURE MATERIALS IN

SUPERCRITICAL CARBON DIOXIDE

H. Saari
Associate Professor
Carleton University
Ottawa, Ontario, Canada
henry.saari@carleton.ca

C. Parks
Research Associate
Carleton University
Ottawa, Ontario, Canada
curtisparks@cmail.carleton.ca

R. Petrusenko
Project Analyst
International Safety Research
Ottawa, Ontario, Canada
petrusenko@i-s-r.ca

B. Maybee
Research Assistant
Carleton University
Ottawa, Ontario, Canada
brennanmaybee@cmail.carleton.ca

K. Zanganeh
Research Scientist
CanmetENERGY
Natural Resources Canada
Ottawa, Ontario, Canada
Kourosh.Zanganeh@NRCan-RNCan.gc.ca

ABSTRACT

Supercritical carbon dioxide closed Brayton cycle power conversion systems are potentially more efficient than plants based on steam cycles for inlet temperatures above 600 °C. They are simpler, more compact, and should therefore be less expensive than conventional steam power plants. However, minimal data exist regarding the corrosive effects of supercritical carbon dioxide at elevated temperatures, which is an important technical concern in the design and material selection of turbomachinery, heat exchangers, piping, and other components that come in contact with this working fluid. In the present study, the design, assembly, and commissioning of a corrosion test rig for conducting long-term studies of potential structural materials and their performance in supercritical carbon dioxide is described. The rig is capable of operating at a maximum vessel temperature of 800 °C (at an internal pressure of 17.5 MPa) and a maximum internal pressure of 29 MPa (at a vessel temperature of 750 °C). Corrosion testing of 316SS, IN718, and IN738 coupons is performed at various levels of temperature and pressure. Coupons are exposed to temperatures of 550 and 700 °C at pressures of 15 and 25 MPa for up to 1500 hours. At each temperature, an additional set of coupons is tested up to 3000 hours (1500 hours at 15 MPa and then up to 1500 hours at 25 MPa). Corrosion response is characterized by weight change measurements and metallography, and is related to alloy composition and testing conditions. All three alloys form a stable protective oxide layer at the lower temperature of 550 °C, while at 700 °C, only IN718 and IN738 form a protective layer.

INTRODUCTION

Supercritical carbon dioxide ($S-CO_2$) Brayton cycles are receiving an increased focus, throughout various sectors, for power conversion due to potential for higher efficiency, smaller footprint, and reduced capital cost, when compared to conventional steam power plants [1]. Through the manipulation of $S-CO_2$ around

and above the critical point, significant gains in thermal efficiency can be found due to the low compressibility of S-CO$_2$. The high efficiency is derived through this characteristic, where a relatively small increase in pressure will result in a large increase in density [1, 2]. As a result, less work is required by the compressor.

With the research and development at Carleton University of S-CO$_2$ Brayton cycle technology, material compatibility became an important area of investigation due to the lack of material testing results that exist for S-CO$_2$ environments. This data is required for the appropriate material selection of components in various pressure and temperature regimes throughout the Brayton cycle. The most recent and relevant testing that has been completed was Gibbs [3] and Dunlevy [4] at the Massachusetts Institute for Technology (MIT), in addition to the research being conducted at Sandia National Laboratories by Wright et al [5] and University of Wisconsin-Madison [6]. Based on the corrosion test rig and results provided by Gibbs and Dunlevy at MIT, a corrosion test rig was commissioned by Carleton University, in collaboration with the Clean Electric Power Generation – Zero-Emission Technologies group at Natural Resources Canada (NRCan).

The work discussed in this paper highlights the design and commissioning of the NRCan-Carleton University corrosion test rig, followed by preliminary test results of candidate alloys for use in an S-CO$_2$ Brayton cycle. The three alloys tested provide an initial investigation of material compatibility, through oxide surface characterization and weight gain trends, of three classes of high temperature alloys: austenitic stainless steel, iron-nickel based superalloys, and nickel based superalloys. The three test alloys, 316SS, IN718, and IN738, in addition to samples of IN625, as outlined in Table 1, were exposed to combinations of pressure and temperature consisting of: 15 MPa/550 °C, 15 MPa/700°C, 25 MPa/550 °C, and 25 MPa/700 °C, for up to a total of 3000 hours. This preliminary testing produced results in the form of weight gain trends, which provides an indication of the relationship of oxide growth to variation in conditions of pressure and temperature.

CORROSION TEST RIG DESIGN

For the purpose of testing candidate materials for a S-CO$_2$ Brayton cycle, the design and construction of a corrosion test rig was commissioned in partnership with the Zero Emission Technology group at Natural Resources Canada (NRCan) [9]. The NRCan-Carleton University corrosion test rig was designed to ASME standards, based on the work described by Dunlevy [4], for primary operating points of 25 MPa/700 °C and 15 MPa/750 °C to align with expected operating conditions within a S-CO$_2$ Brayton cycle. It was to operate at flow rates of at least 1 L/hr, nearly autonomously, with passive and active safety features to prevent over pressurization and excessive temperatures. The preliminary design of the rig was performed at Carleton University by Petrusenko [9], with the final detail design done by Pressure Vessel Engineering Ltd., Waterloo, Ontario for Canadian Registration Number (CRN) designation.

A process and instrumentation diagram (P&ID) of the NRCan-Carleton University corrosion test rig can be found in Figure 1. The rig is an autoclave design, where all samples are loaded into the pressure vessel via an alumina specimen boat. The rig is continuously supplied with CO$_2$ of at least 99.9% purity, capable of flow rates ranging from 0.5-15 L/hr. Supplied from a bulk storage tank, CO$_2$ enters the two-stage gas booster at a pressure of 1.52 MPa after passing through a 15.0 μm particulate filter. The CO$_2$ is then routed through a 7 μm filter to a 300 mL buffer tank used to dampen pressure fluctuations caused by the cycling gas booster. Before the pressure vessel, the CO$_2$ encounters the pressure relief valve, rupture disk, and pressure transducer. A number of thermocouples are positioned on the exterior of the pressure vessel, in addition to probes inserted from both ends of the pressure vessel, which provide temperature measurements approximately 5 cm from both ends of the specimen boat. All instrumentation signals were read and recorded using a Graphtec GL820 data logger. A provision exists for integration of a residual gas analyzer to record the composition of supplied and exhausted CO$_2$ to monitor any change in composition.
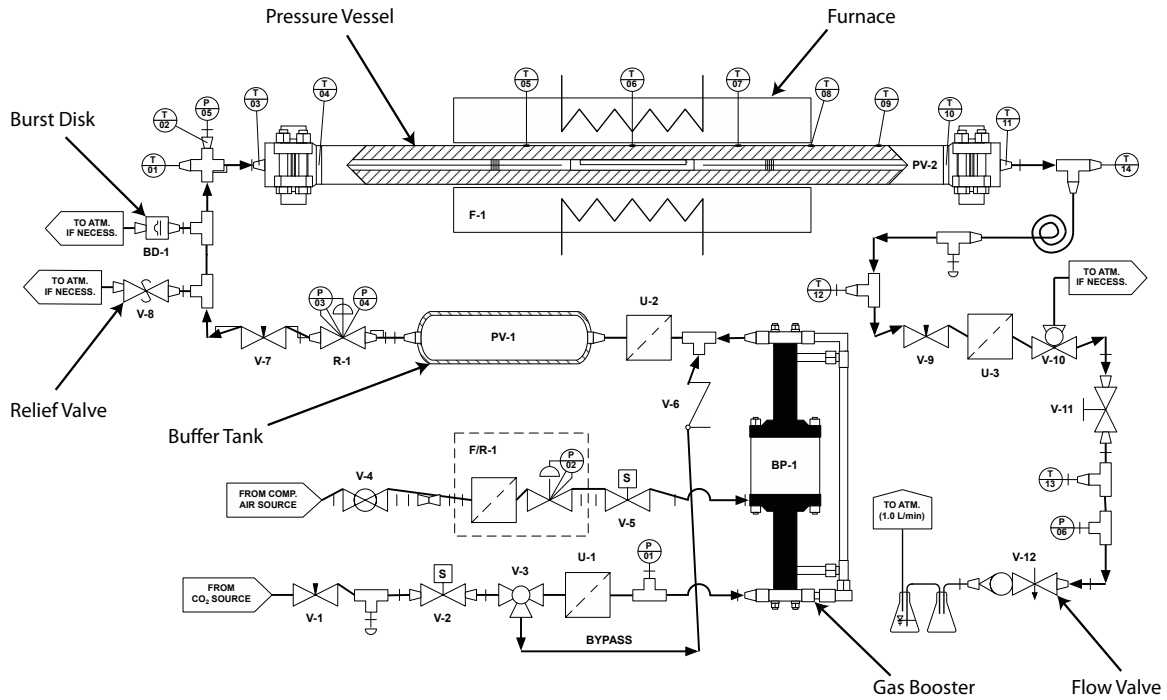
Figure 1: Corrosion test rig piping and instrumentation diagram (P&ID).

The main components of the rig, instrumental for effective operation include: the pressure vessel, gas booster, furnace, integrated safety features, and the specimen boat. In the design stage, the pressure vessel was originally considered to be made of IN617, IN625, or Haynes 230. IN625 was eventually selected based on the favourable corrosion performance test results from MIT and UW-Madison, in addition to machinability and cost.

Figure 2: NRCan-Carleton University corrosion test rig.

A gas booster was selected for the pressurization of the rig. The SC Hydraulic Engineering Corp GBT-15/30 two-stage gas booster is driven using compressed air, where the output pressure is governed by a gas amplification factor based on pressure and flow capacities of the given CO_2 and air sources.

3

For the heating of the pressure vessel, a Thermcraft Inc. CST-6-0-24-3V furnace was selected. The furnace provides three independently controlled zones with a cumulative power output of 6800 W. The zones are controlled using a Thermcraft Inc. 3-1-40-230-E15SP control system, which guides the heating of each zone to a desired set point at a predetermined rate of 200 °C/hour. Set points have been determined through commissioning trial runs for specific test points to achieve uniform temperature distribution throughout the test section inside the vessel.

In order to ensure that the integrity of the pressure vessel would never be compromised even under most unexpected temperature and pressure conditions, in addition to acquiring Technical Standards and Safety Authority (TSSA) approval for the entire rig, multiple safety features were integrated into the design. These three main features included: a pressure relief valve, solenoid valves, and rupture disk, which were triggered in sequence at predetermined conditions outlined in Figure 3.
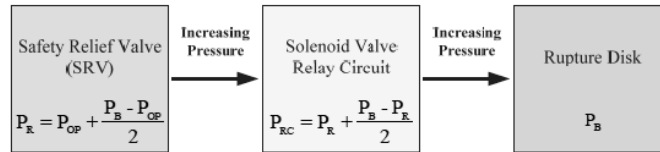
Figure 3: Corrosion rig active safety features priority sequence where P_R is relief pressure, P_{OP} is operating pressure, P_B is burst pressure, and P_{RC} is circuit activation pressure [9].

As a first line of defence against overpressure, the relief valve would automatically open at either 16.32 MPa or 27.21 MPa, depending on the desired operating pressure of 15 MPa or 25 MPa. In the event the relief valve is not effective at reducing the pressure of the pressure vessel, a solenoid valve relay circuit would be triggered at a pressure of 16.99 MPa or 28.31 MPa, which would close the flow of air and CO_2 into gas booster. The solenoid valve relay circuit, which uses normally closed solenoid valves, controlled through a normally-open relay, would also isolate the gas booster from its supply lines in the event of an electrical power failure. Finally, the rupture disk would open at a pressure of either 17.65 or 29.41 MPa.

Placement of the test coupons was facilitated through the use of an alumina specimen boat, shown in Figure 4, which suspended and electrically isolated the samples in the center of the pressure vessel. The specimen boat was designed to accommodate coupons 12.7 mm in diameter, which are separated form each other using alumina washers. The configuration was designed from four pieces of alumina to save costs and was fabricated by Elan Technology of Midway, Georgia. The boat measures 266.7 mm in length, with a 3.2 mm diameter alumina rod for hanging the specimens, and incorporates a semi-circular void at each end to encourage flow across the coupons.

The specimen boat is loaded into the pressure vessel through the end opening, which is sealed with 316SS Grayloc flanges. Based on heat transfer analysis, it was determined that the temperatures at the end of the IN625 vessel were low enough to use 316SS Grayloc flanges. A flange was welded to each end of the IN625 vessel and was sealed with a blind Grayloc hub. A NPT threaded hole was drilled in the center of each hub to allow for a thermocouple to feed through on each end.
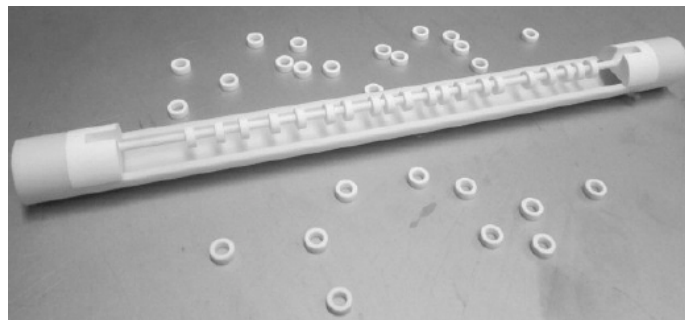
Figure 4: Alumina specimen boat used to suspend test coupons in the corrosion test rig. The alumina washers shown are used to separate and space the test coupons [9].

CORROSION TEST RIG COMMISSIONING

Commissioning tests were performed to assess the functionality and performance of the rig against the original design requirements [9]. The main objectives of these tests were to verify the correct operation of the rig, to determine appropriate furnace set points for the various test temperatures, and to confirm the repeatability of achieving the desired test conditions. In accordance with the desired testing conditions that match the extremes within a S-CO$_2$ Brayton cycle, the rig was tested at 15 and 25 MPa and at 50 °C increments between 550 and 700 °C.

A profile thermocouple with six measurement locations centered in the test region of the pressure vessel was used throughout the commissioning tests. This thermocouple provided readings for the temperature profile that the specimen boat would experience in the test region. Furthermore, thermocouples placed on the exterior of the pressure vessel provide measurements of metal temperature along the length of the vessel. The rig was operated to determine the appropriate furnace set points that would result in uniform temperature distribution along the length of the specimen boat, for each of the desired test temperatures at both 15 and 25 MPa. The furnace controller was set to increase temperature at a rate of 200 °C/hour, chosen to minimize thermal shock to the system. Once at the initial set temperature, the found set points were determined by altering the controller set points and observing the changing internal temperature profile. This was done until the temperatures along the length of the specimen boat position were close to the desired test temperature. Subsequently, verification testing was done to confirm repeatability of the set points.
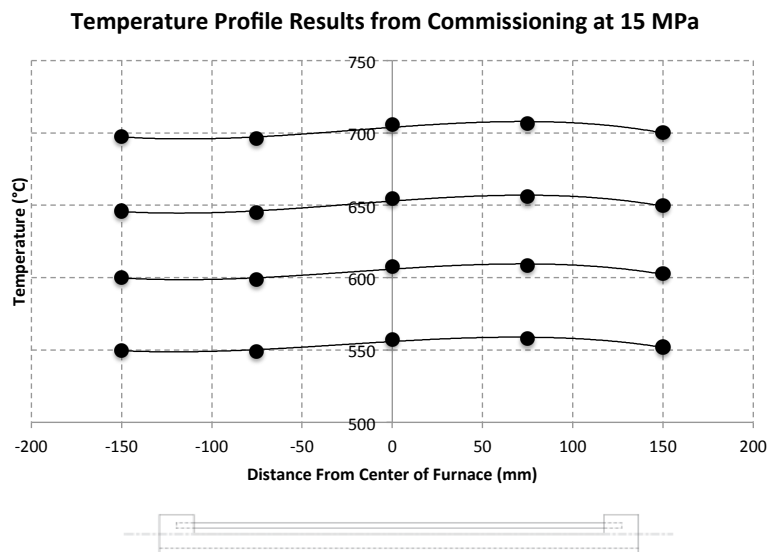
Figure 5: Temperature profile within pressure vessel for various test temperatures at 15 MPa [9].

During initial commissioning, it was found that a large amount of heat was lost throughout the length of the vessel, resulting in a large temperature gradient across the length of the test region. As a result, molybdenum disks were added, attached to the thermocouple probes, to act as heat reflectors. Molybdenum was used, as there was a supply of spare heat shield material readily available, so the addition of the heat reflectors could be implemented rapidly, and not delay the test rig commissioning. Five disks were used on each side of the test region, located at the edges of the heated zones. These were crimped on to each thermocouple probe, and were spaced using 6.35 mm thick alumina washers. The disks were also perforated to allow for flow of the S-CO$_2$. The addition of the heat reflectors resulted in a significant decrease in the maximum change in temperature across the test region in the pressure vessel. Figure 5 displays the temperature profiles within the test region, with respect to the specimen boat, after the addition of the heat reflectors. For the length of the specimen boat where the coupons are located (i.e. approximately the middle 150 mm of the boat) the maximum temperature variation is 10 °C. For 700 °C testing, the range is 696-706 °C, and for 550 °C it is 549-557 °C.

After the commissioning tests at 15 MPa, further commissioning was done at 25 MPa to assess proper operation and determine the appropriate furnace set points for the higher test temperature. The change in thermal conductivity of S-CO_2 at the higher pressure became evident, as the rig required significantly higher set points to achieve the same temperature. On average, the rig was approximately 40 °C cooler when at 25 MPa than at 15 MPa using the same furnace set points [9].

TEST DESIGN

The preliminary testing that was conducted with the corrosion test rig was designed as an initial investigation of three different types of candidate materials for use in a supercritical carbon dioxide Brayton cycle [10]. Following the design parameters of the Carleton University Brayton cycle Loop (CUBCL), four combinations of pressure and temperature were selected to closely represent the extreme operational conditions within the cycle. Furthermore, the test conditions were chosen to examine the dependence on pressure and temperature for oxide growth and ability to form a protective oxide. The four test points that were chosen consisted of combinations of 550 °C and 700 °C at 15 MPa and 25 MPa.

As an initial investigation of material compatibility with S-CO_2, the three different types of alloys that were tested included: austenitic 316SS, iron-nickel-based IN718, and nickel-based IN738. The nominal composition for each is provided in Table 1. Together these three classes of alloys represent the material options for various components through the Brayton cycle loop, from compressor and turbine turbomachinery, to piping and valve assemblies. The results of this initial testing would provide guidance for more extensive testing and evaluation techniques of candidate materials.

Table 1: Nominal composition of test alloys [7,8].

Alloy	Cr	Ni	Co	Mo	Nb	Ti	Al	Fe	C	Other
625	21.5	61	-	9.0	3.6	0.2	0.2	2.5	0.05	-
718	19	52.5	-	3	5.1	0.9	0.5	18.5	0.08	Cu
738	16	61.5	8.5	1.75	2	3.4	3.4	-	0.17	Zr,B,W
316	16-18	10-14	-	2-3	-	-	-	Bal	0.08	Mn, Si, P, S

The initial testing examined the weight gain characteristics of the aforementioned alloys up to 3000 hours of exposure. In an effort to capture the initial kinetics of oxide growth, test time intervals were chosen as: 100, 250, 500, 1000, and 1500 hours. At each time interval, the test coupons were removed from the specimen boat, weighed, and photodocumented. One coupon from each sample set was also removed and stored for future analysis. The overall results provided a sample for every combination of pressure and temperature, for each time interval up to 3000 hours. Furthermore, to examine the corrosion performance of the pressure vessel, which was manufactured from IN625, two coupons of this alloy were added to the test matrix in addition to the three main test alloys.

As the corrosion test rig was designed to accommodate 12.7 mm test coupons, they were manufactured from 12.7 mm (½") bar stock of each test alloy. They were designed for a high surface-area-to-volume ratio to maximize the proportion of oxide-to-alloy weight, which would be measured using a balance with a readability of 0.01 mg. A total of 30 coupons of each test alloy were manufactured with a diameter of 12.7 mm and a thickness of approximately 1.2 mm. Based on an investigation of typical surface roughness specifications of as-delivered alloys, the coupons were prepared to a surface roughness of 600-grit to closely simulate the expected surface roughness of manufactured components. The final steps of coupon preparation involved drilling a 4 mm hole for hanging the coupons in the specimen boat, and labeling the coupons using a metal engraver. Each sample was labeled with a 3-digit number consisting of: 1XX for 316SS, 2XX for IN718, 3XX for IN738, and 4XX for IN625. The last two digits ranged from 1-30 for the specific coupon identifier. An example of a prepared coupon is illustrated in Figure 6.

12.7 mm

Figure 6: Example of prepared test coupon number 216.

To capture and have the ability to examine the dependence on pressure and temperature, six sample sets of five coupons each, were required. Each test began with two sample sets of each alloy in the specimen boat. The first test condition was 550 °C and 15 MPa. At each time interval, a coupon was removed from one sample set of each alloy. After 1500 hours, an entire sample set of each alloy had been removed, and a new sample set of each was added for the next 1500 hours of testing at 25 MPa. After a total of 3000 hours, the testing resulted in a sample set that had either been exposed to only 550 °C/15 MPa or only 550 °C/25 MPa for 1500 hours, or a combination of 15 MPa and 25 MPa over 3000 hours. Testing was then repeated using the remaining three sample set of each alloy, except at 700 °C instead of 550 °C. This test matrix is illustrated in Table 2.

Table 2: Test matrix.

Temp (°C)	Exposure Time (hours)					
	316SS		IN718		IN738	
	15 MPa	25 MPa	15 MPa	25 MPa	15 MPa	25 MPa
550	1500		1500		1500	
550	1500 + 1500		1500 + 1500		1500 + 1500	
550		1500		1500		1500
700	1500		1500		1500	
700	1500 + 1500		1500 + 1500		1500 + 1500	
700		1500		1500		1500

Coupons were systematically removed from testing to minimize the dependence on location with the specimen boat or pressure vessel. This process consisted of removing the first coupon in the specimen boat at the first time interval, and then the last coupon at the next. This process continued until an entire sample set had been removed, and the new sample set was placed in the vacant positions.

RESULTS AND DISCUSSION

The preliminary results of the initial corrosion tests consisted of cumulative weight gain plots as a function of exposure time, and oxide layer metallography of several coupons. The weight gains of individual test coupons were recorded and are shown in Figure 7, with the weight gain values normalized by the surface area of the coupon. In Figure 7, the solid lines indicate the coupons that were exposed at 15 MPa for up to 1500 hours, and then at 25 MPa in the range from 1500 to 3000 hours. The dashed lines indicate the coupons that were exposed at 25 MPa for up to 1500 hours. The dotted lines show the results for the two IN626 coupons. At 550 °C, the IN625 coupons were exposed at 15 MPa for 1500 hours and then at 25 MPa for 1500 hours. The same two IN625 coupons were then exposed at 700 °C at 15 MPa for 1500 hours and at 25 MPa for 1500 hours. For the 700 °C plots, the cumulative weight gains for the IN625 coupons are relative to their final weight gains after exposure to 550 °C and 15 MPa/25 MPa for a total of 3000 hours. The results shown in Figure 7 indicate the scatter in the measurements at each time interval, as well as the variability associated in the weight gains of individual coupons. Some of the scatter and variability can result from the fact that the weight gains measured were typically on the order of the resolution of the balance that was used. Also, the oxide layer may have been damaged during coupon handling, or exposure to moist air between tests may have caused some of the scatter. In addition to weight gain plots for individual coupons, the weight gains for all coupons were averaged at each

7

measurement interval. The plots of these averaged values are shown in Figure 8 (for the different test temperatures) and in Figure 9 (for the different test pressures) as the curves of best fit through the data.

The three plots on the left hand side of Figure 7 are for the alloys at 550 °C. The 316SS and IN718 coupons showed similar weight gain trends when compared to each other. However, IN738 coupons had approximately half the weight gain of 316SS and IN718. The IN625 coupons showed slightly lower weight gain when compared to 316SS and IN718. Comparing IN625 to IN738, up to 1500 hours the weight gains were comparable, but from 1500 to 3000 hours IN625 exhibited higher weight gain. In general, protective oxide layers can be interpreted through a parabolic growth rate law resulting from the decreasing rate of oxide formation. A stable and adherent oxide provides a barrier that inhibits further ion diffusion, slowing the formation of new oxide. A logarithmic rate law, which is purely an empirical relationship with no fundamental underlying mechanism, would also indicate a protective oxide layer. This would typically be seen with thin oxide layers that form at relatively lower temperatures. In contrast, unprotective oxide layers are unable to prevent or slow the formation of new oxide, and can be interpreted through a linear oxide growth rate law. Under these circumstances, the oxide could be coarse, porous, cracked, non-adherent to the substrate, which would continually provide for new areas for anion and cation reactions to take place [11,12]. Overall, at 550 °C, all three alloys tested seem to exhibit logarithmic oxide growth kinetics, as shown in Figure 8. In this figure, the best-fit curves, through the data averaged at each measurement interval, are logarithmic.

The three plots on the right hand side of Figure 7 are for the alloys at 700 °C. The IN718 and IN738 coupons showed similar weight gain trends when compared to each other, while the 316SS coupons showed dramatically higher weight gains. The IN625 coupons showed lower weight gains when compared to IN718 and IN738. However, it should again be noted that the cumulative weight gains of the IN625 coupons are relative to the weight gains of those coupons after the "pre-exposure" to the 550 °C testing. As shown, by the best fit curves through the averaged data in Figure 8, 3166 exhibited linear oxide growth characteristics while both IN718 and IN738 exhibited parabolic oxide growth characteristics. These results indicate that the oxide layer that forms on 316SS in unstable and unprotective, while the oxide layers that form on IN718 and IN738 are both stable and protective. In all cases, the test coupons exposed at 700 °C exhibited higher cumulative weight gains, and thus faster oxide growth rates, than the test coupons exposed at 550 °C.

While the effect of test temperature on weight gain trends is quite clear from Figures 7, 8, and 9, the effect of test pressure is generally less apparent. At 550 °C, for both 316SS and IN718, it appears that the initial (up to approximately 250-500 hours of testing) and final weight gains are generally higher for exposure at 15 MPa as compared to 25 MPa. However, for IN738, it seems that testing at 25 MPa resulted in slightly higher weight gains, as compared to 15 MPa. At 700 °C, for all alloys it appears that testing at 25 MPa results in a higher initial weight gain. For 316SS, the weight gain remains higher up to 1500 hours of testing. However, for IN718 and IN738 it appears that the weight gains at 1500 hours for both 15 and 25 MPA approach the same magnitude. Also, for the testing at 700 °C, it appears that there is a slight "uptick" in the weight gains for all alloys at 1500 hours, when the pressure was increased to 25 MPa. This "uptick" is not as apparent in the testing at 550 °C. So, in general, there does seem to be some dependence of weight gain on the test pressure with a higher pressure resulting in increased weight gain, at least initially (i.e. for the first 250-500 hours or testing, or shortly after the test pressure was increased). However, this did not hold for all tests, where 316SS and IN718 at 550 °C showed lower weight gain at 25 MPa when compared to 15 MPa. The reason for this behaviour is not clear.
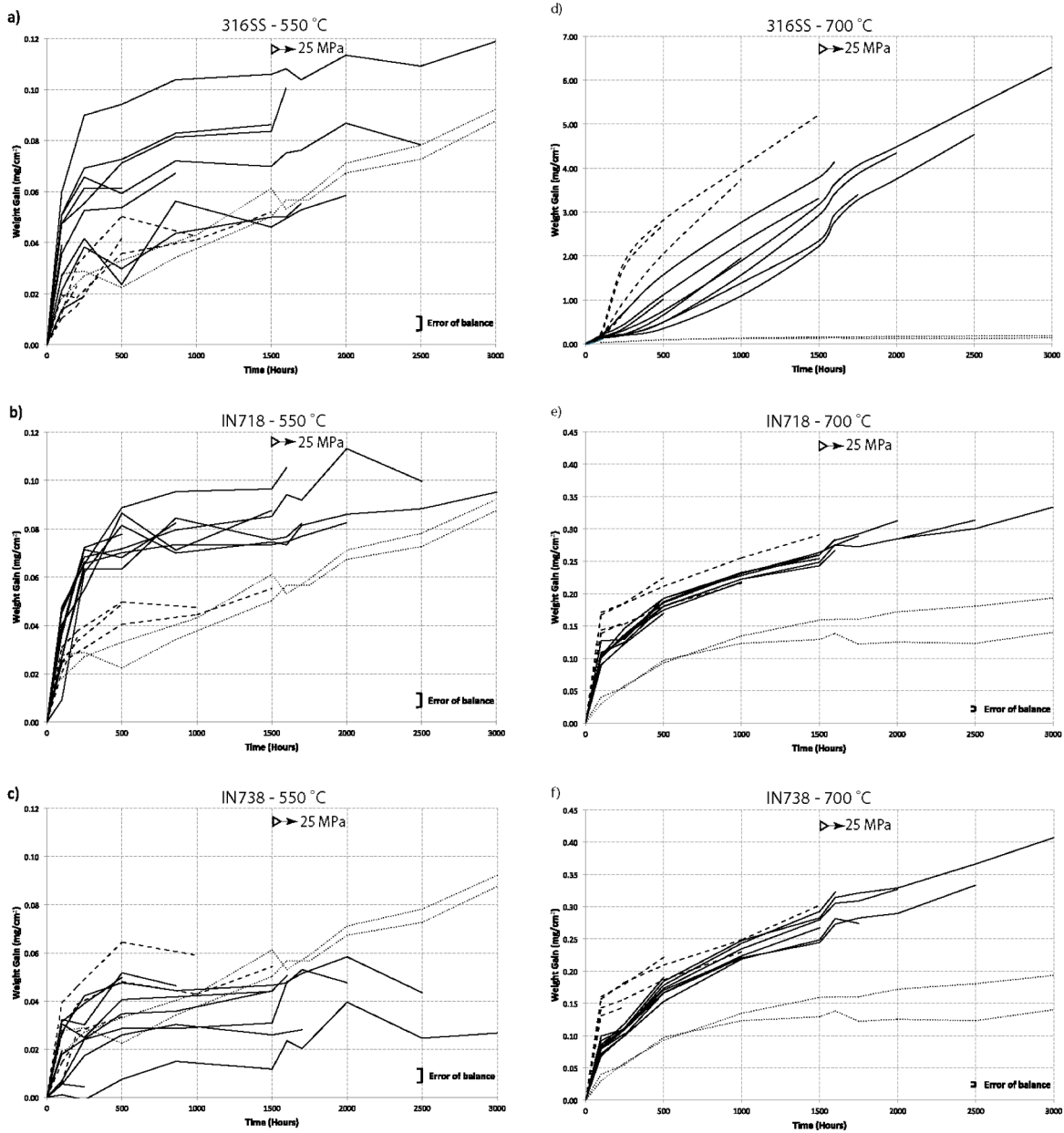
Figure 7: Weight gain of individual coupons at 550 °C and 700 °C. The solid lines are samples exposed to 15 MPa up to 1500 hours, and then 25 MPa from 1500-3000 hours. The dashed lines are samples exposed to 25 MPa for up to 1500 hours. The dotted line represent IN625 coupons tested when under the same conditions. Note that the weight gains for IN625 coupons at 700 °C are relative to the cumulative weight gain after the testing at 550 °C. Also note the different vertical axis scale.

9

a)

316SS

Change in Mass (mg/cm²)

6.00

5.00

4.00

25/700
y = 0.0037x
R^2 = 0.94992

3.00

15/700
y = 0.0019x
R^2 = 0.98931

2.00

1.00

15/550, 25/550
y = 0.013ln(x) - 0.0195
R^2 = 0.9534

0.00

0   250   500   750   1000   1250   1500

Exposure Time (Hours)

b)

IN-718

Change in Mass (mg/cm²)

0.35

0.30

☐ Error of balance

0.25

25/700
y = 0.0543x^0.2189
R^2 = 0.92856

0.20

y = 0.021x^0.3432
R^2 = 0.99171
15/700

0.15

15/550
y = 0.0173ln(x) - 0.0379
R^2 = 0.86908

0.10

25/550   y = 0.01ln(x) - 0.019
R^2 = 0.94499

0.05

0.00

0   250   500   750   1000   1250   1500

Exposure Time (Hours)

c)

IN-738

Change in Mass (mg/cm²)

0.35

0.30

☐ Error of balance

0.25

y = 0.0426x^0.2572
R^2 = 0.95024
25/700

0.20

y = 0.0094x^0.4597
R^2 = 0.98549
15/700

0.15

0.10

25/550
y = 0.0114ln(x) - 0.0272
R^2 = 0.95187

0.05

y = 0.0065ln(x) - 0.01
R^2 = 0.79786
15/550

0.00

0   250   500   750   1000   1250   1500

Exposure Time (Hours)

Figure 8: Weight change comparison of 316SS, IN718, and IN738 based on temperature. The plotted data at each time interval is an average of the coupons measured for each alloy. Temperature and pressure are indicated by MPa/ °C. The dashed line represents weight change values for the first 1500 hours at 15/550 of IN625.   Note that the representative error for Figure 8 a) is too small to display.
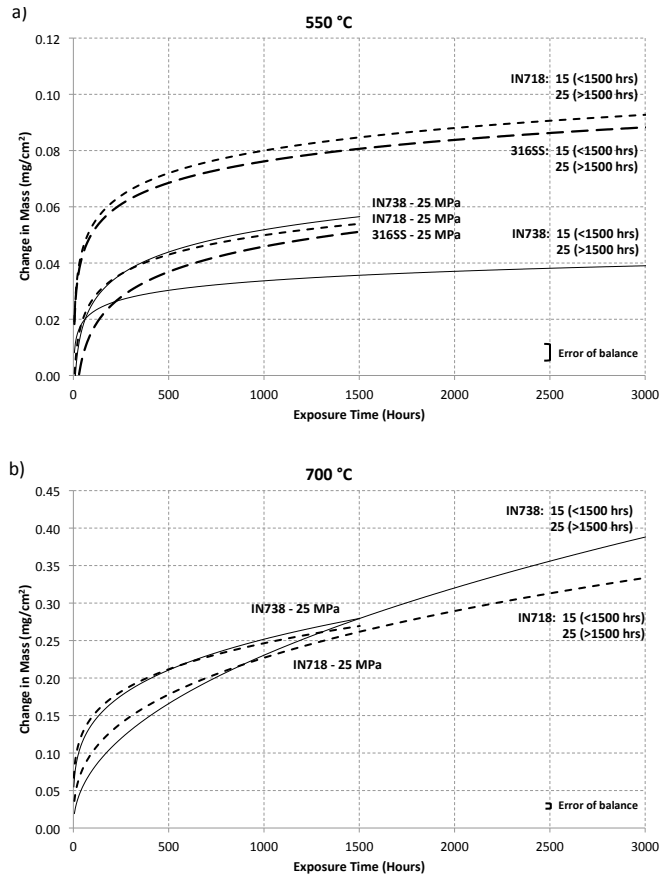
Figure 9: Weight change comparison for 316SS, IN718, and IN738 coupons based on pressure for testing up to 3000 hours. The plotted values represent the average for each time interval for each alloy.

A preliminary analysis on samples tested at 700 °C was conducted using a Scanning Electron Microscope (SEM), with results shown in the micrographs in Figure 10. Corresponding with its linear oxide growth rate, 316SS exhibits an unstable, duplex oxide layer. In comparison, the much thinner and more stable oxide layer found for IN718 is characteristic of a protective oxide layer, although there is some evidence of intergranular corrosion. Evidence of intergranular corrosion is more apparent for IN738. However, from the weight gain trends, the oxide layer is still providing adequate protection up to 3000 hours. Based on the micrograph of IN738, this oxide would be expected to fail after further advancement of the intergranular corrosion depleting the substrate of ions.
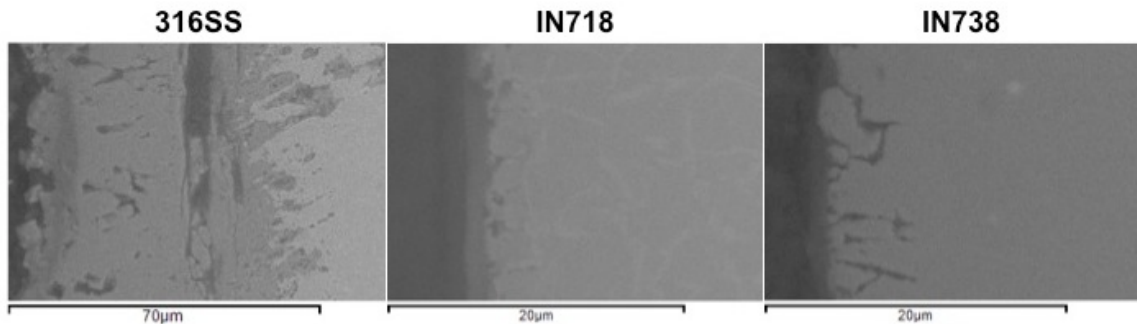
Figure 10: Micrographs of 316SS, IN718, and IN738 after 1500 hours of exposure at 700 ˚C/15 MPa then 1500 hours at 700 ˚C/25 MPa.

11

Conclusions

For the purpose of investigating material compatibility of high temperature alloys in S-CO$_2$, the corrosion test rig developed through collaboration with Carleton University and NRCan was found to be an adequate tool in providing preliminary data on the corrosion resistance of materials exposed to elevated temperature S-CO$_2$. The design of the rig, which was built on the success of Gibbs [3] and Dunlevy [4], was manufactured and commissioned for the purpose of evaluating materials under conditions ranging from 15 and 25 MPa and 550-750 °C. The operation of the rig was validated through commissioning tests with the original design parameters. Furnace set points were determined through this testing and confirmed repeatability for predetermined temperature and pressure set points.

The three test alloys, 316SS, IN718, and IN738, were exposed to combinations of 15/25 MPa and 550/700 °C for up to 3000 hours, where weight change measurements were recorded at time intervals of 100, 250, 500, 1000, and 1500 hours. At the lower temperature of 550 °C, all three alloys performed exceptionally well at both pressures by producing a protective oxide layer, with logarithmic growth kinetics. The oxide produced from each alloy was stable and effective at slowing or preventing further diffusion of ions for the formation of new oxide. However, at the higher temperature of 700 °C, the performance of 316SS deteriorated severely.

At the higher test temperature of 700 °C, 316SS was unable to produce a protective oxide layer, which was evident from the linear oxide growth kinetics. This high rate of oxide formation corresponds to the inability to slow the rate of ion diffusion and the formation of new oxide. This high rate of formation increased with the higher test pressure of 25 MPa.

In contrast, IN718 and IN738 both performed reasonably well under testing at 700 °C and 15/25 MPa. Both alloys exhibited parabolic oxide growth kinetics, considered protective due to the gradual decrease in new oxide formation. The high pressure of 25 MPa resulted in a more rapid oxide formation within the initial 250 hours of testing but the total weight gain eventually merged with the 15 MPa results after 1500 hours.

Overall, based on the preliminary data discussed, all three test alloys provide adequate qualities for use within S-CO$_2$ at conditions limited to 550 °C. The results indicate that 316SS is not suitable for applications of 700 °C due to unstable oxide growth. The superalloys tested, IN718 and IN738, show promise in use under all tested conditions based on stable oxide growth rates, but further metallographic analysis is required to verify the compatibility with S-CO$_2$, in addition to longer term testing to evaluate consequences of intergranular corrosion.

Acknowledgements

REFERENCES

[1]   Dostal, V., 2004. "A Supercritical Carbon Dioxide Cycle for Next Generation Nuclear Reactors." Massachusetts Institute of Technology.

[2]   Wright, S.A., Conboy, T.M., Rochau, G.E. 2011. "Overview of Supercritical CO2 Power Cycle Development at Sandia National Laboratories." Sandia National Laboratories.

[3]   Gibbs, J.P., 2011. "Corrosion of Various Engineering Alloys in Supercritical Carbon Dioxide." Massachusetts Institute of Technology.

[4]   Dunlevy, M.W., 2009. "An Exploration of the Effect of Temperature on Different Alloys in a Supercritical Carbon Dioxide Environment." Massachusetts Institute of Technology.

[5]   Wright, I.G., Thimsen, D., 2013. "Materials Considerations for Supercritical CO2 Turbine Cycles." GT2013-94941, ASME Turbo Expo 2013.

[6]   Sridharan, K., Anderson, M., Jelinek, J. et al., 2011.   "Corrosion of Candidate Alloys in High Temperature Supercritical Carbon Dioxide." University of Wisconsin, Madison.

[7]   Donachie, M.J., Donachie, S.J., 2002.   "Superalloys – A Technical Guide, 2nd ed." ASM International.

[8]   Davis, J.R., 2010. "Concise Metals Engineering Data Book, 5th ed." ASM International.

[9]   Petrusenko, R.G., 2011.   "The Development of a High Temperature Supercritical Carbon Dioxide Corrosion Test Rig." Carleton University.

[10]   Parks, C.J., 2013. "Corrosion of Candidate High Temperature Alloys in Supercritical Carbon Dioxide." Carleton University.

[11]   Mattsson, E., 1996. "Basic Corrosion Technology for Scientists and Engineers, 2nd ed." IOM Communications.

[12]   Binks, N., Heier, G.H., Pettit, F., 2006. "High Temperature Oxidation of Metals." New York: Cambridge University Press.